

Myobolica: A Stochastic Approach to Estimate Physiological Muscle Control Variability

Alex Bersani[®], Mercy Amankwah, Daniela Calvetti[®], Erkki Somersalo[®], Marco Viceconti[®], and Giorgio Davico[®]

Abstract—The inherent redundancy of the musculoskeletal systems is traditionally solved by optimizing a cost function. This approach may not be correct to model non-adult or pathological populations likely to adopt a "non-optimal" motor control strategy. Over the years, various methods have been developed to address this limitation, such as the stochastic approach. A well-known implementation of this approach, Metabolica, samples a wide number of plausible solutions instead of searching for a single one, leveraging Bayesian statistics and Markov Chain Monte Carlo algorithm, yet allowing muscles to abruptly change their activation levels. To overcome this and other limitations, we developed a new implementation of the stochastic approach (Myobolica), adding constraints and parameters to ensure the identification of physiological solutions. The aim of this study was to evaluate Myobolica, and quantify the differences in terms of width of the solution band (muscle control variability) compared to Metabolica. To this end, both muscle forces and knee joint force solutions bands estimated by the two approaches were compared to one another, and against (i) the solution identified by static optimization and (ii) experimentally measured knee joint forces. The use of Myobolica led to a marked narrowing of the solution

Manuscript received 27 May 2024; revised 26 July 2024; accepted 14 August 2024. Date of publication 22 August 2024; date of current version 11 September 2024. This work was supported by the European Commission through the H2020 Project "In Silico World: Lowering Barriers to Ubiquitous Adoption of In Silico Trials" (topic SC1-DTH-06-2020) under Grant 101016503. The work of Giorgio Davico was supported by the European Commission through the European Union—NextGenerationEU funded by the Italian Ministry of University and Research under Piano Nazionale di Ripresa e Resilienza (PNRR)—M4C2-I1.3 Project PE_00000019 "Health Extended ALliance for Innovative Therapies, Advanced Lab-Research, and Integrated Approaches of Precision Medicine (HEAL ITALIA)" to Marco Viceconti under Grant CUP J33C22002920006. (Corresponding author: Alex Bersani.)

Alex Bersani and Giorgio Davico are with the Department of Industrial Engineering, Alma Mater Studiorum-University of Bologna, 40126 Bologna, Italy (e-mail: alex.bersani2@unibo.it; giorgio.davico@unibo.it).

Mercy Amankwah was with the Department of Mathematics, Applied Mathematics and Statistics, Case Western Reserve University, Cleveland, OH 44106 USA (e-mail: mga26@case.edu).

Daniela Calvetti and Erkki Somersalo are with the Department of Mathematics, Applied Mathematics and Statistics, Case Western Reserve University, Cleveland, OH 44106 USA (e-mail: dxc57@case.edu; ejs49@case.edu).

Marco Viceconti is with the Department of Industrial Engineering, Alma Mater Studiorum-University of Bologna, 40126 Bologna, Italy, and also with the Medical Technology Laboratory, Rizzoli Orthopaedic Institute, 40136 Bologna, Italy (e-mail: marco.viceconti@unibo.it).

This article has supplementary downloadable material available at https://doi.org/10.1109/TNSRE.2024.3447791, provided by the authors. Digital Object Identifier 10.1109/TNSRE.2024.3447791

band compared to Metabolica. Furthermore, the Myobolica solutions well correlated with the experimental data ($R^2=0.92$, RMSE = 0.3 BW), but not as much with the optimal solution ($R^2=0.82$, RMSE = 0.63 BW). Additional analyses are required to confirm the findings and further improve this implementation.

Index Terms— Suboptimal control, muscle recruitment, stochastic approach, Markov chain Monte Carlo, OpenSim.

I. INTRODUCTION

EDUCTIONISM in biomechanics favors the separation between biomechanics and neurology of human movement. The number of muscles that the central nervous system may choose to produce the same movement is considerably higher than the number of degrees of freedom of a human body (defined by the body's allowed movement); this discrepancy results in a redundancy situation for the muscular system [1], where the muscle activation patterns that may be selected to reach the same goal are essentially endless. Traditionally, the biomechanics community tended to reduce the complexity of neuromuscular control with the assumption that among all possible control strategies that satisfy the physical and physiological constraints, the central nervous system will choose one minimizing some cost functions representative of a physiological criterion (reductionist approach) [2]. With this assumption, musculoskeletal dynamics models can predict the muscle activation patterns given measured kinematics plus ground reactions using inverse dynamics and static optimization [3]. Several studies have confirmed that this is an acceptable approximation for healthy adults who perform sub-maximal stereotypical tasks such as level walking [4], [5]. Unfortunately, much biomechanics research focuses on pathological subjects whose neuromuscular control deviates more or less significantly from this assumption (sub-optimal control).

Several approaches have been proposed to overcome this limitation [6] such as electromyography(EMG)-based [7], [8], [9], [10] and feedback-based approaches [11]. A different approach was proposed in [12], where the problem of constrained control was formulated in terms of Bayesian statistics, and a Markov Chain Monte Carlo (MCMC) algorithm was used to sample the solution space of all muscle activation patterns that satisfy the dynamic equilibrium and the tetanic limits. Instead of searching for an optimal solution, we sampled all possible solutions using a software implementation called *Metabolica*, originally developed for analyzing

metabolic networks [13]. The advantage of this approach is that it does not rely on the EMG information and makes no assumption of synergies, thus considering also the least optimal muscle activation patterns. The Metabolica approach was successfully used in studies where the question was how sub-optimal control could increase joint loading [14], [15], [16], [17].

However, Metabolica assumes that each instant of the locomotion cycle is independent of the others; the solution space is built assuming instantaneous equilibrium without concern about whether a muscle was already activated or not in the previous instant. However, this is not physiologically correct: a muscle cannot abruptly change its activation level (and therefore its force).

The aim of this study was to evaluate whether the neuromuscular control variability predicted assuming as constraints only the equilibrium of forces and moments and the tetanic limit for each muscle (i.e., Metabolica approach [13]) changed (and to which extent) when the muscle force generation velocity was accounted for. We named this new approach Myobolica and hypothesized that it would narrow the solution band (compared to Metabolica), including only the more physiologically plausible estimates.

The reader is referred to [18] for a mathematical dissertation on the Myobolica approach.

II. MATERIAL AND METHODS

A. Experimental Data

The experimental data used in this study, which include motion capture, ground reaction forces, and in vivo knee contact forces measured with an instrumented implant on an 83-year-old male subject, are part of the sixth Grand Challenge Competition dataset [19] In particular, the first available overground gait trial (DM_ngait_og3) was selected for our case study and processed to ensure that a full gait cycle was included, i.e., that the first and last frames corresponded to two consecutive right heel strikes on the force plate.

B. Musculoskeletal Model

A personalized single-leg musculoskeletal model was employed to perform the simulations. The model, built off the available post-operative medical imaging data of the subject under study, was inherited from previous work [20] and included 5 bodies (pelvis, femur, patella, tibia, and foot), 11 degrees of freedom (3 for the hip, 1 for the knee and the ankle, 6 connecting the model to the ground) and 43 muscle-tendon actuators.

C. OpenSim Workflow - Optimal Solution

The open-source software OpenSim (v4.1) [21] was used to estimate joint kinematics and kinetics, as well as the musculoskeletal parameters such as the muscle lever arms. The OpenSim's static optimization tool was then employed to predict the 'optimal' and reference solution, i.e., set of muscle forces and activation patterns, that minimized the sum of squared muscle activations [22], henceforth referred to as optimal solution, and the resulting total knee joint contact forces (JCF).

D. Stochastic Approach

Stochastic simulations were performed with Metabolica and Myobolica through MATLAB (v2021b), setting the number of solutions to be identified to 8×10^5 . This number was deemed sufficient considering that in previous studies where Metabolica was employed such value was set to 1×10^5 and 2×10^5 , respectively [12], [17].

Once the solutions had been generated, the knee JCFs were predicted by leveraging on the OpenSim API for MATLAB (similarly to what was done to compute the JCFs corresponding to the optimal solution).

Of note, in Metabolica no manifold was applied, i.e., the solution space was not restricted, and the sampler could explore the entire space of solutions.

The mathematical concepts behind Myobolica and the rationale and procedure to select the key parameters defining how it works (Table I) are summarized in the following sections. For a complete description of the mathematics behind Myobolica, we refer the reader to [18].

E. Myobolica - Equilibrium Condition

The Myobolica tool considers muscle forces as random variables based on observations on joint torques and muscle moment arms (1) and a priori information to constrain muscle forces (2):

$$M = B \times F_{\text{mus}} + \varepsilon \tag{1}$$

$$F_{\min} \le F_{\max} \le F_{\text{tetanic}}$$
 (2)

where B is the matrix of muscle lever arms, M is the joint torques vector, F_{mus} is the unknown muscle forces vector bounded between its minimum value (F_{min}) and maximum value ($F_{tetanic}$). The parameter ε models noise and uncertainties as Gaussian white noise:

$$\varepsilon \sim N(0, \sigma^2 In)$$
 (3)

By adopting a Bayesian statistics methodology, Myobolica describes the unknown muscle forces vector as a posterior Probability Distribution Function (PDF):

$$\pi(F_{\text{mus}}|M) \propto \pi \operatorname{pr}(F_{\text{mus}})\pi(M|F_{\text{mus}})$$
 (4)

where $\pi(F_{mus}|M)$ is the posterior PDF of the muscle forces, $\pi_{pr}(F_{mus})$ is the prior PDF and $\pi(M|F_{mus})$ is the likelihood.

Sigma (σ) is the parameter modeling noise and uncertainties in the equilibrium condition equation, and it represents the standard deviation of the Gaussian PDF in (3). To define a plausible range for the σ parameter we estimated the error ε (1) by propagating the experimental error of the instrumented knee prosthesis adopted in our example dataset [19].

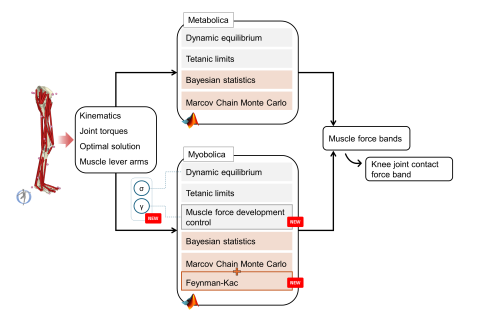
F. Myobolica – Muscle Force Development Velocity Control

The classical formulation for the Bayesian statistic (adopted in Metabolica) would assume that PDFs at different time-frames are mutually independent. This lacks physiological accuracy – due to the natural limits of the muscle activation velocity (and, as a result, of the muscle force development

Modeling of uncertainties in equilibrium equation

Myobolica Parameters Defined for This Case Study		
Parameter	Value	Description
Samples	800000	Number of solutions to be identified
Step analyzed	2^{nd}	Reduce the dependence on the optimal solution

TABLE I MYOBOLICA PARAMETERS DEFINED FOR THIS CASE STUD



Sigma

Gamma

0.12

0.0022

Fig. 1. Summary of the workflow done. Firstly, biomechanical parameters are extracted from the musculoskeletal model. Then, an implementation of the stochastic approach is executed (Myobolica or Metabolica). In the end, both implementations provide as output a band of plausible muscle forces, in turn used to compute a band of plausible knee JCF profiles. In Myobolica, σ and γ are parameters related to uncertainties modeling and the new "yank" constraint and the mutual independency among frames is reached through the Feynman-Kac model path sampling.

velocity); in other words, different timeframes cannot be mutually independent. To overcome this, in Myobolica, we modeled the concept of "yank", which is the time derivative of a muscle force [23]. In particular, we defined the yank as a PDF:

$$F_{\text{mus},t} - F_{\text{mus},t-1} = \eta t \tag{5}$$

$$\eta t = N(0, \gamma^2) \tag{6}$$

Modeling the yank binding through this prior PDF – discussed in detail in [18] – allows us to compute a solution that keeps track of each simulation timeframe information. Notably, the sampling of longitudinal paths rather than single solutions (required to obtain solutions which respect the new yank constraint) is achieved through the Feynman-Kac model [24]. Briefly, the Feynman-Kac path formalism (developed for diffusion-type parabolic equations) introduces a probability distribution in the space of path over time and represents solutions as expectation of integrals over paths similarly to how in our modelling problem the muscle force posterior PDF is defined by the yank prior PDF [18].

Gamma (γ) represents the standard deviation of the Gaussian PDF describing the yank variance (6). In particular, γ (which controls the yank) relates to an experimental parameter frequently measured or estimated in experimental muscle characterization studies: the rate of force development (RFD), at times reported as the rate of moment/torques development (RMD). The RFD describes the capacity of a muscle to rapidly generate force [25] and is measured in Newton per second [N/s] (or Nm/s, when derived from torques). The RFD is calculated during maximal voluntary isometric contraction tests (MVIC tests) of sports gestures for athlete's performance evaluation or constrained to an instrumented chair in the clinical environment. Commonly, the parameter is estimated

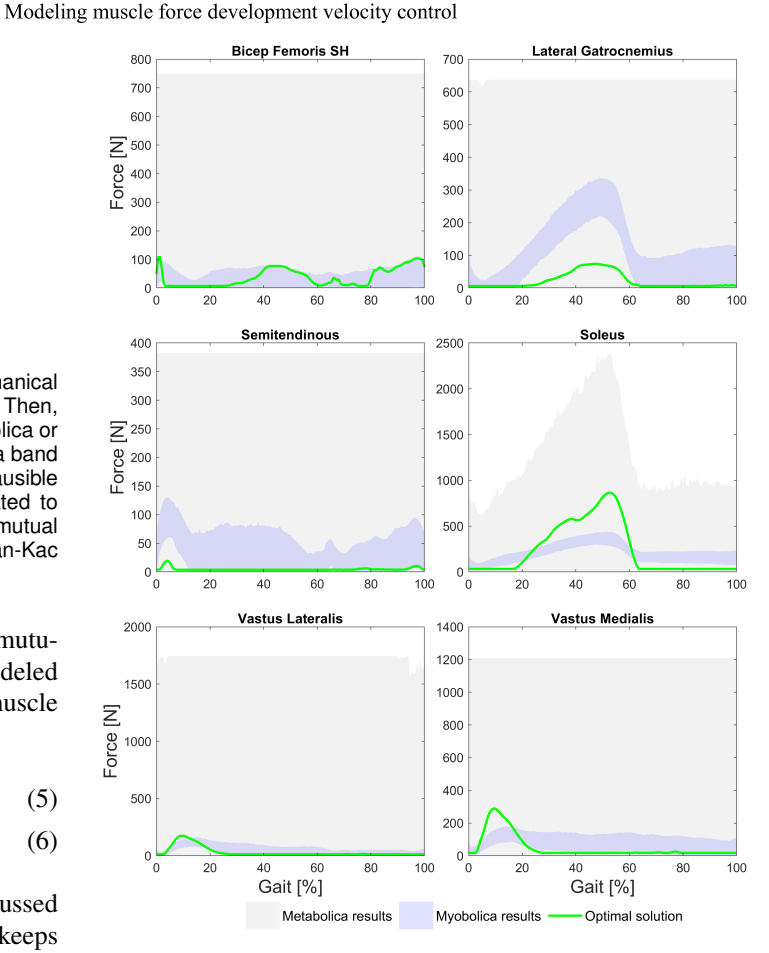


Fig. 2. Muscle force solutions bands comparison between Myobolica (blue) and Metabolica (grey). The optimal solution is plotted in green.

during the first 300-400 ms of the executed task [25] and clustered into shorter intervals.

G. Myobolica - Consecutive Steps Analysis

To run, Myobolica requires a first tentative solution (i) to compute an early value of the muscle force development velocity control and (ii) to define the initial conditions at the first timeframe of the simulation (the initial set of muscle forces).

To limit the dependency of the Myobolica solutions on the tentative solution, which corresponds to the optimal solution from static optimization, we simulated two consecutive steps. More specifically, assuming that the kinematics variability between steps is little to negligible [26], the median muscle force patterns among the Myobolica solutions estimated after the first run were provided as tentative solutions for the simulation of the second step. In addition, the pool of plausible initial conditions to guide the initial sampling for the second step was set to the values of the Myobolica solutions at the last timeframe of the first step.

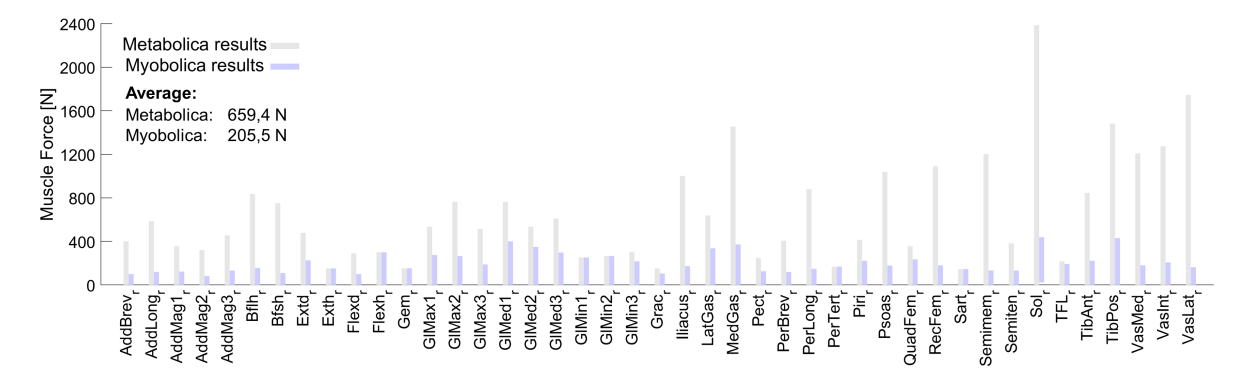


Fig. 3. Comparison of muscle range of forces estimated by Myobolica (blue) and Metabolica (grey).

Henceforth, with the term Myobolica solutions we refer to the solutions of the second step.

H. Data Analysis

A schematic summary of the work done in this paper is reported in Fig. 1. For both Myobolica and Metabolica, the resulting solution space (i.e., set of muscle forces) was initially sorted in ascending order to facilitate the identification of the minimum and maximum solutions, along with the 10th, 25th, 75th, and 90th percentiles as well as the median solution. Similarly, the estimated knee JCF profiles were first normalized to the subject's body weight and then sorted in ascending order.

The comparison between the results from Metabolica and Myobolica is performed employing descriptive statistics and similarity metrics (i.e., R² and root mean square error - RMSE) as well as through the quantification of the range of variation (min to max solution), further complemented by a qualitative analysis.

In addition, the Myobolica solution space was compared to the optimal solution and to the experimental knee JCFs (i) measuring the overlap (as percentage, throughout time), (ii) computing the R² and RMSE, and (iii) comparing the ranges of variation.

III. RESULTS

For clarity and to keep the Results section concise, we hereby only report the results for a subset of muscles, i.e., *triceps surae*, *vastii*, and *hamstrings* (see Fig. 2). Additional comparisons and results may be found in the Appendix.

Overall, the inclusion of an additional constraint (yank parameter) to control the force-generating capability of a muscle when exploring the solution space through a stochastic approach (i.e., Myobolica implementation) led to a significantly narrower solution band compared to the output from Metabolica (previous implementation of the stochastic approach where no manifold was applied and the solutions at consecutive frames were independent of one another, thus allowing for abrupt changes in muscle force).

On average, the bandwidth (spectrum of solutions) across all modeled muscles was 659.4 N for Metabolica and 205.5 N for Myobolica (see Fig. 3). More specifically, for the *soleus* muscle, the force range estimated by Metabolica was 2385.7 N,

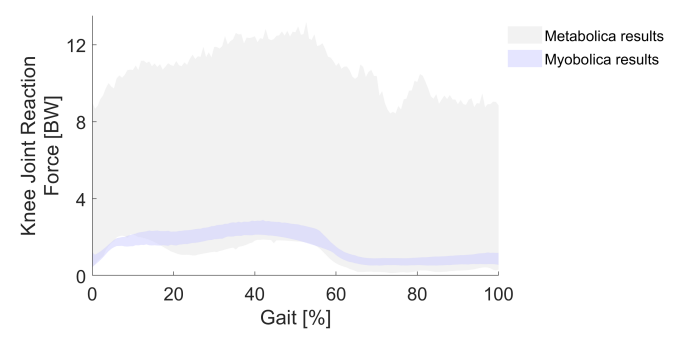


Fig. 4. Comparison of knee JCF solution bands estimated by Myobolica (blue) and Metabolica (grey).

compared to 415.3 N from Myobolica; for the *vastus medialis* 1207.7 N compared to 180.2 N; for the *medial gastrocnemius*, 1454.1 N compared to 371.7 N.

Similarly, the spectrum of the knee JCFs – computed from the identified set of muscle forces – ranged from 0.45 BW to 2.9 BW in Myobolica (see Fig. 4) and from 0.14 BW to 13.2 BW in Metabolica, with an average solution variability of 0.6 BW for Myobolica and 9.7 BW for Metabolica.

From a qualitative assessment, for both approaches, the peak force was observed at around 55% of the gait cycle (in correspondence of the typical second characteristic peak of knee JCF force in a walking trial). The profiles of the solution spaces between Myobolica and Metabolica were similar in shape ($R^2=0.87$, RMSE = 4.5 BW, between the medians of the two solution bands). In S.Fig.1 a comparison between muscle activation solution bands estimated by Myobolica and the experimental EMG signals is provided.

Compared to the true value, i.e., data from the instrumented knee implant, the Myobolica solution band showed a high correlation level ($R^2 = 0.92$ and RMSE = 0.3 BW, between Myobolica median solution and experimental JCF profile). Furthermore, the implant data were almost completely enclosed in the solution space identified by Myobolica (for approximately 72.8% of the gait cycle; see Fig. 5).

By contrast, the knee JCF resulting from the optimal solution identified via the classical static optimization approach (Fig. 5, green line), thus hypothesizing optimal muscle control, was characterized by a first characteristic peak larger than the second characteristic peak (i.e., overall maximum identified around initial heel contact, at \sim 8% of the gait cycle, compared to \sim 55% in both the experimental data and the Myobolica

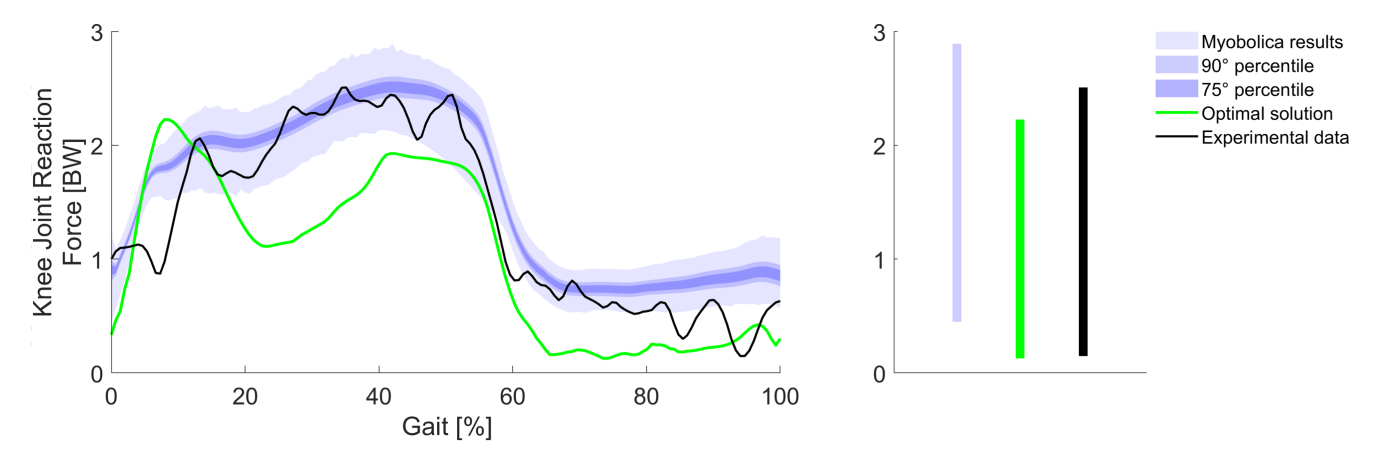


Fig. 5. Comparison of knee JCF estimated by Myobolica (blue shade bands), optimal solution (green) and experimentally measured data (black). Right: min-to-max range of the solutions estimated by the two methods and the experimentally measured value.

solutions). Shape-wise, the optimal solution was not as similar to the Myobolica band of solutions as the implant data (i.e., $R^2 = 0.82$, RMSE = 0.63 BW, between the medians of Myobolica solutions band and the optimal solution), and fell mostly outside of it (i.e., 15.9% overlap across the gait cycle).

IV. DISCUSSION

The aim of this paper was twofold: to present the results of Myobolica, a tool to implement a stochastic approach to predict physiologically plausible muscle forces and activation patterns accounting for neuromuscular control variability while constraining the ability of muscles to rapidly generate force, and to compare the obtained variability to the variability predicted assuming as constraints only the equilibrium of forces and moments and the tetanic limit for each muscle (i.e., Metabolica).

As hypothesized, introducing a term to discourage abrupt changes in muscle force led to a marked narrowing in the solution band (in terms of knee joint contact forces, from 13 BW to 2.4 BW, Fig. 3 and Fig. 4), compared to results from Metabolica [12], [13]. While part of the solution space obtained with Metabolica may be considered physically plausible as the identified solutions satisfy both the dynamics of the system (equilibrium) and the tetanic limits of the muscles (i.e., maximal isometric force values), those same solutions may not be physiologically plausible. In fact, when the γ parameter (to control the yank) was introduced, a large portion of the Metabolica solution space was no longer explored (Fig. 4). This may suggest that even in a subject adopting a suboptimal control (such as the subject under study), some variability in neuromuscular control is physiological, but it may be less than previously hypothesized.

In addition, the knee joint contact force profiles calculated from the solution space identified by Myobolica more closely approximated the experimental data from the instrumented implant. This may be reconducted to the higher muscle-co-contraction resulted by Myobolica. The introduction of the γ and σ parameters to control the yank and the uncertainties in the equilibrium condition, respectively, had thus a twofold (positive) effect: to reduce the band of solutions and to enable more accurate predictions. Interestingly, the optimal solution (generated hypothesizing optimal muscle control – i.e.,

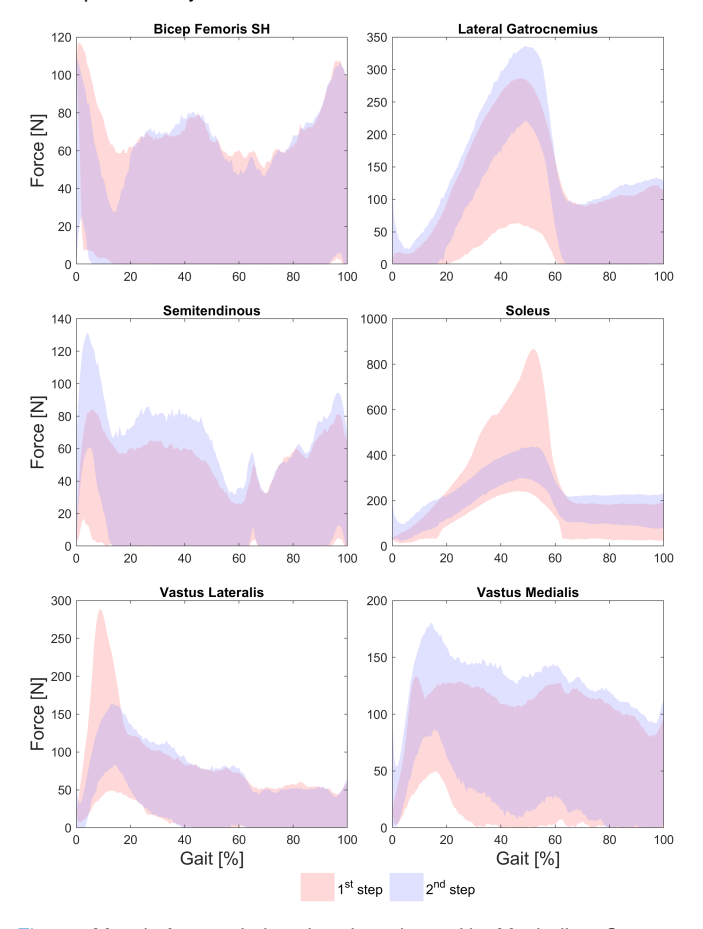


Fig. 6. Muscle force solutions bands estimated by Myobolica. Comparison of the first (red) and the second (blue) simulated step.

minimization of sum squared muscle activations) is close to but not comprised within the range of Myobolica solutions. This circumstance calls for further investigation.

The authors are aware of the limitations of this work. For instance, the computational cost is non-negligible. While a single Myobolica solution (i.e., set of muscle forces and activations plus the resulting knee joint contact force) can be generated in as little as 0.3 seconds, the overall time required to compute the whole band of solutions (e.g., 8×10^5 solutions) is in the order of hours due to a lack of parallelization in

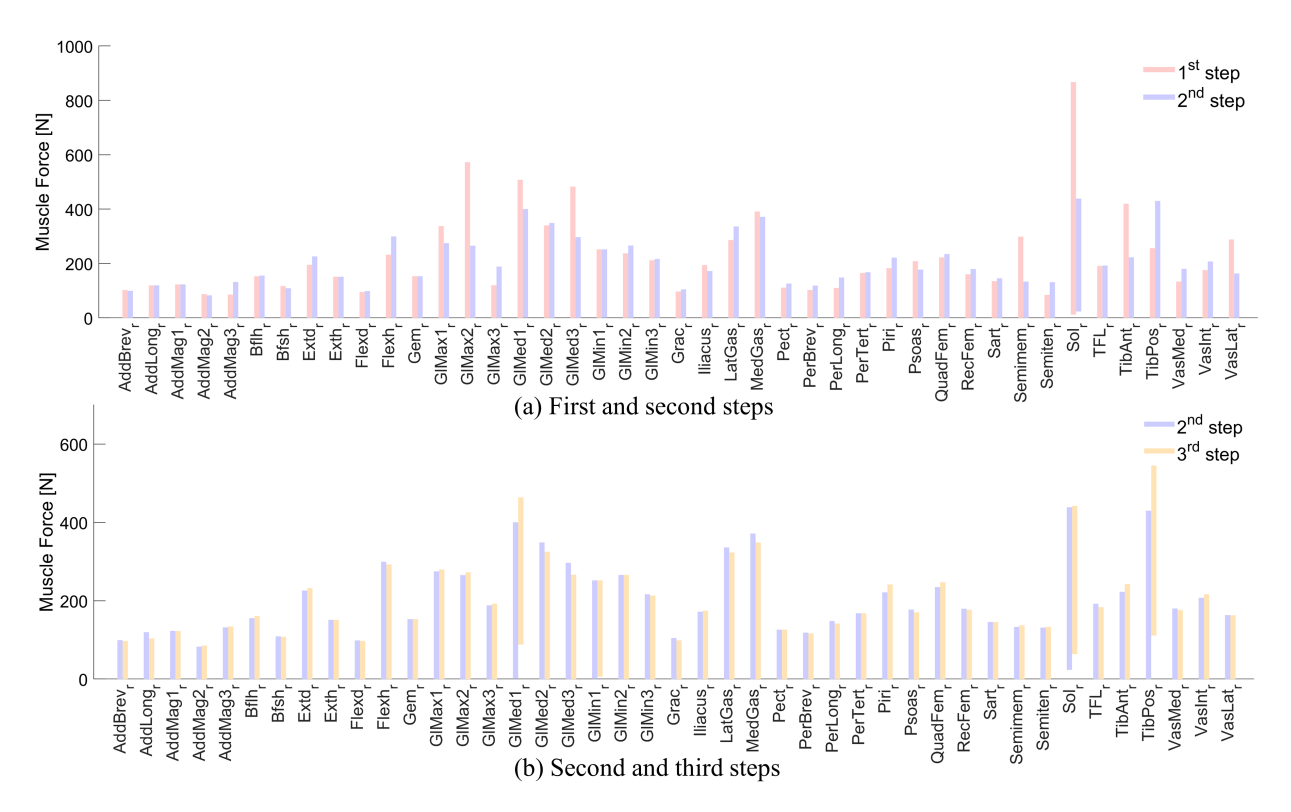


Fig. 7. Comparison of muscle range of forces estimated by Myobolica. In (a), comparison between the first (red) and second (blue) simulated step; in (b), comparison between the second (blue) and third (orange) simulated step.

the current implementation. Moreover, the γ parameter – related to the yank control – may vary between populations, with significant differences between trained and untrained subjects. Additional tests should be performed to study the effect of such parameters on different subjects. The authors point out that this paper was conducted on one subject with an explorative purpose, and the set γ parameter was comparable to values found in the literature.

The analysis of more subjects is planned in the near future to confirm the conclusions the authors drew in this document, along with a sensitivity analysis to quantify the effect of the values assigned to γ and σ (hereby carefully selected, but likely different depending on the characteristics of the population) and a convergence analysis to identify the minimum number of solutions to be sampled and consecutive steps to be performed to minimize the computational cost.

If future analysis will confirm results emerged in this study, new application scenarios may be hypothesized where the stochastic approach could be used to enhance "what if" kind of study and provide an extended band of what the subject is able to do (in terms of muscle forces) given the kinematics and the subject specific muscle condition.

APPENDIX A TOOLBOX PARAMETERS

The study for the definition of physiological ranges for Myobolica governing parameters was accomplished for two we defined "gamma" (γ) and "sigma" (σ) .

To define a physiological range for the γ parameter we estimated the rate of moment development (RMD) from data collected in our laboratory on 31 people (both young and old

individuals. ClinicalTrials ID: NCT05795348, NCT05854316 [27]) who performed maximal voluntary isometric contraction (MVIC) tests of the lower limbs on a Biodex System 4 Pro isokinetic dynanometer (Biodex Medical System, New York, NY, USA).

The experimental results (i.e., computed RMDs) were clustered into 3 intervals based on the selected analysis window: 0-50 ms, 0-100 ms, 0-200 ms. No specific cluster was chosen, and the results were pooled together, as the peak performance reached in a MVIC test (experimental task) is unlikely to be reached during an overground walk (simulated task). The values thus extracted were in line with the literature [25], [28], [29], [30], [31], [32].

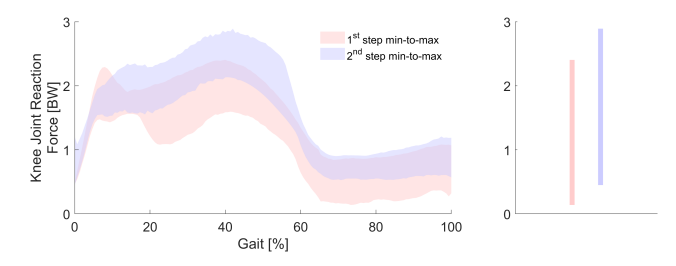
The computed RMDs were later scaled to the timescale of the employed simulation data (in our case, 0.008334 seconds):

$$RMD_{scaled} = RMD \times \Delta t_{specific}$$
 (A1)

As in Myobolica the yank is described as a Gaussian PDF with average value and standard deviation respectively equal to 0 and γ , to ensure all yank values are described by the Gaussian distribution (the authors remind the reader that 99.7% of the values lie within 3 times the standard deviation) we modelled the γ parameter starting from the average RMD value typical of elderly subjects, as in (A2):

$$3 \times \gamma > RMD_{experimental}$$
 (A2)

where RMD_{experimental} was the RMD normalized to the measured peak torques and scaled to the simulation timescale. The overall largest value (across clusters) was selected.



Comparison of the knee JCFs estimated by Myobolica in the first (red) and in the second (blue) simulated step.

The purpose of normalization is to enable comparison of results across studies where different motor tasks are studied.

To define a plausible range for the σ parameter we estimated the error ε (1) by propagating the experimental error of the instrumented implant worn by the subject under study [19]:

$$\varepsilon_{\text{Force,knee}} = \sum_{i=1}^{\text{Nmuscles}} k_i(t) \cdot \varepsilon_{\text{Force,i}}(t)$$

$$k_i(t) = \frac{F_{\text{mus,i}}(t)}{F_{\text{knee,resultant}}(t)}$$
(A3)

$$k_{i}(t) = \frac{F_{\text{mus,i}}(t)}{F_{\text{knee.resultant}}(t)}$$
(A4)

where $\varepsilon_{Force,knee}$ is the maximum absolute error measured during the calibration of the instrumented prosthesis [33] i.e., about 1% of the maximum value measured during trial acquisition.

Assuming that the contribution of each muscle to the knee joint force (and so to the error of that measure) is proportional to the force generated by the same muscle, we defined $\varepsilon_{\text{Force,knee}}$ as a linear combination of muscle force errors $(\varepsilon_{\text{Force},i})$ weighted by their contribution to the knee resultant force (A3). The contribution k_i was set to 0 for muscles not insisting on the knee joint.

The joint torque error ε was estimated propagating the muscle force error $\varepsilon_{Force,i}$ in (1):

$$M + \varepsilon = B \times [F_{\text{mus}} + \varepsilon_{\text{Force mus}}]$$
 (A5)

This way, an ε value for each simulation time frame was estimated, and the biggest one, around the second peak of the gait cycle ε reached the value of 0.36 Nm, was chosen as reference value.

To ensure noise and uncertainties in (1) to be described by a Gaussian distribution with average value 0 and standard deviation σ , we modelled the σ parameter starting from the previously described ε :

$$3 \times \sigma > \varepsilon$$
 (A6)

APPENDIX B STEP SELECTION

The analysis of a second consecutive step is mainly motivated by the need to obtain a solution independent from the initial optimal solution, but it led to the estimation of a significantly different solution space. To explore how the periodization of the gait cycle could affect the outcome, a third consecutive step was simulated searching for differences in the resulting solution spaces between the second and the third steps. The median muscle activation pattern estimated in the second cycle is assigned as required tentative solution in the third one and the last timeframe's solution of the second gait

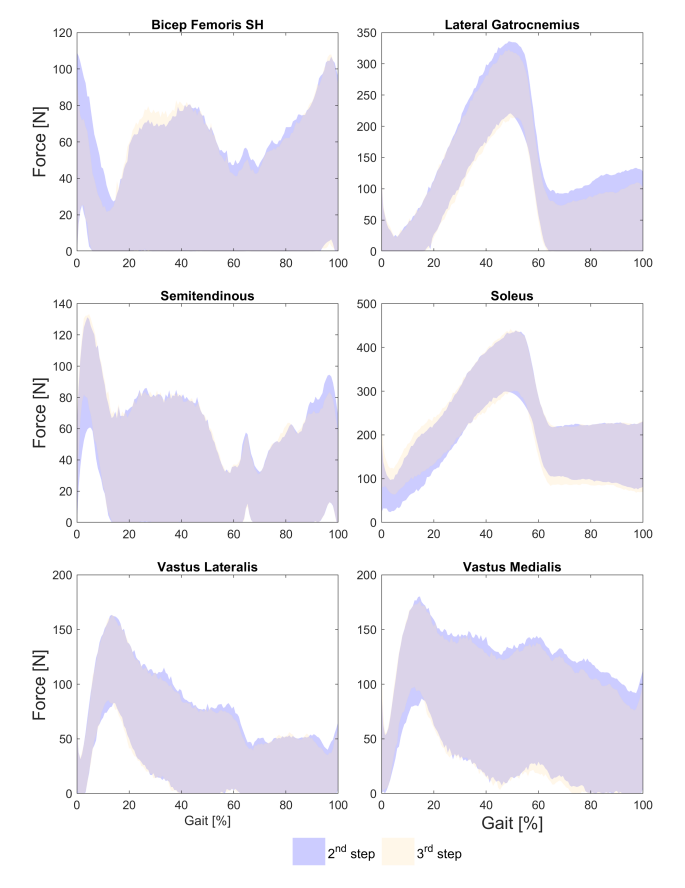


Fig. 9. Muscle force solutions bands estimated by Myobolica. Comparison of the second (blue) and the third (orange) simulated step.

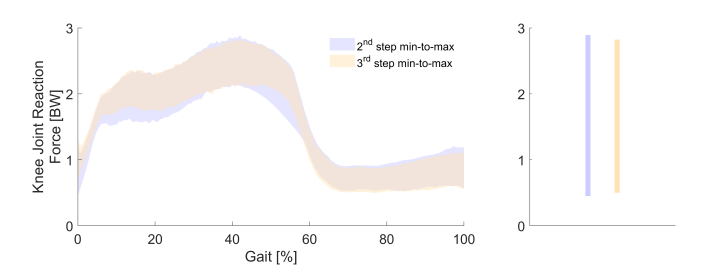


Fig. 10. Comparison of the knee JCFs estimated by Myobolica in the second (blue) and in the third (orange) simulated step.

cycle is carried out as the pool of plausible initial conditions for the third gait cycle.

The comparison between the Myobolica solution for the first and second steps is shown in A.Fig. 6. The average muscle force range across muscles is 226.7 N in the first step and 205.5 N in the second step. The largest difference was found for the soleus muscle (from 855.5 N in the first to 415.3 N in the second step. A.Fig. 7(a)).

While the knee joint force solution spaces resemble $(R^2 = 0.97 \text{ and } RMSE = 0.28 \text{ BW between medians of})$ the two solution bands) with force estimated in the first step generally lower than the one estimated in the second one (A.Fig. 8); in the first step, the estimated spectrum ranged from 0.14 BW to 2.4 BW while in the second step from 0.45 BW to 2.9 BW.

Further tests have been performed to determine whether simulating a third step would lead to much different estimates (A.Fig. 9). No significant differences emerged when comparing individual muscle bands (the largest difference emerged for the tibialis posterior bandwidth: from 429.9 N in the second to 434.8 N in the third step. A.Fig. 7(b)). Similarly, the knee joint force solution spaces were very much alike ($R^2 = 0.99$ and RMSE = 0.04 BW between medians of the two solution bands. A.Fig. 10).

Considering the computational time to complete a simulation, the authors deemed the difference between the results from the second and the third step not to be significant enough to require a third step to be performed.

ACKNOWLEDGMENT

The views and opinions expressed are those of the authors only and do not necessarily reflect those of the European Union or the European Commission. Neither the European Union nor the European Commission can be held responsible for them.

REFERENCES

- N. Bernstein, The Co-ordination and Regulation of Movements. Oxford, U.K.: Pergamon Press, 1967.
- [2] A. Seireg and R. J. Arvikar, "A mathematical model for evaluation of forces in lower extremeties of the musculo-skeletal system," *J. Biome-chanics*, vol. 6, no. 3, pp. 313–326, May 1973, doi: 10.1016/0021-9290(73)90053-5.
- [3] A. Pedotti, V. V. Krishnan, and L. Stark, "Optimization of muscle-force sequencing in human locomotion," *Math. Biosciences*, vol. 38, nos. 1–2, pp. 57–76, Jan. 1978, doi: 10.1016/0025-5564(78)90018-4.
- [4] R. Beckett and K. Chang, "An evaluation of the kinematics of gait by minimum energy," *J. Biomechanics*, vol. 1, no. 2, pp. 147–159, Jul. 1968, doi: 10.1016/0021-9290(68)90017-1.
- [5] R. L. Waters and S. Mulroy, "The energy expenditure of normal and pathologic gait," *Gait Posture*, vol. 9, no. 3, pp. 207–231, Jul. 1999, doi: 10.1016/s0966-6362(99)00009-0.
- [6] A. Bersani, G. Davico, and M. Viceconti, "Modeling human suboptimal control: A review," J. Appl. Biomechanics, vol. 39, no. 5, pp. 294–303, Oct. 2023, doi: 10.1123/jab.2023-0015.
- [7] A. H. Caillet, A. T. M. Phillips, D. Farina, and L. Modenese, "Estimation of the firing behaviour of a complete motoneuron pool by combining electromyography signal decomposition and realistic motoneuron modelling," *PLOS Comput. Biol.*, vol. 18, no. 9, Sep. 2022, Art. no. e1010556, doi: 10.1371/journal.pcbi.1010556.
- [8] D. G. Lloyd and T. F. Besier, "An EMG-driven musculoskeletal model to estimate muscle forces and knee joint moments in vivo," *J. Biomechanics*, vol. 36, no. 6, pp. 765–776, Jun. 2003, doi: 10.1016/s0021-9290(03)00010-1.
- [9] S. M. McGill, "A myoelectrically based dynamic three-dimensional model to predict loads on lumbar spine tissues during lateral bending," J. Biomechanics, vol. 25, no. 4, pp. 395–414, Apr. 1992, doi: 10.1016/0021-9290(22)90259-4
- 10.1016/0021-9290(92)90259-4.

 [10] C. Pizzolato et al., "CEINMS: A toolbox to investigate the influence of different neural control solutions on the prediction of muscle excitation and joint moments during dynamic motor tasks,"

 J. Biomechanics, vol. 48, no. 14, pp. 3929–3936, Nov. 2015, doi: 10.1016/j.jbiomech.2015.09.021.
- [11] H. Geyer and H. Herr, "A muscle-reflex model that encodes principles of legged mechanics produces human walking dynamics and muscle activities," *IEEE Trans. Neural Syst. Rehabil. Eng.*, vol. 18, no. 3, pp. 263–273, Jun. 2010, doi: 10.1109/TNSRE.2010.2047592.
- [12] S. Martelli, D. Calvetti, E. Somersalo, M. Viceconti, and F. Taddei, "Computational tools for calculating alternative muscle force patterns during motion: A comparison of possible solutions," *J. Biomechanics*, vol. 46, no. 12, pp. 2097–2100, Aug. 2013, doi: 10.1016/j.jbiomech.2013.05.023.
- [13] J. Heino, D. Calvetti, and E. Somersalo, "Metabolica: A statistical research tool for analyzing metabolic networks," *Comput. Methods Programs Biomed.*, vol. 97, no. 2, pp. 151–167, Feb. 2010, doi: 10.1016/j.cmpb.2009.07.007.

- [14] K. J. Bennett et al., "EMG-informed neuromusculoskeletal models accurately predict knee loading measured using instrumented implants," *IEEE Trans. Biomed. Eng.*, vol. 69, no. 7, pp. 2268–2275, Jul. 2022, doi: 10.1109/TBME.2022.3141067.
- [15] S. Martelli, D. Calvetti, E. Somersalo, and M. Viceconti, "Stochastic modelling of muscle recruitment during activity," *Interface Focus*, vol. 5, no. 2, Apr. 2015, Art. no. 20140094, doi: 10.1098/rsfs.2014.0094.
- [16] B. C. van Veen, C. Mazza, and M. Viceconti, "The uncontrolled manifold theory could explain part of the inter-trial variability of knee contact force during level walking," *IEEE Trans. Neural Syst. Rehabil. Eng.*, vol. 28, no. 8, pp. 1800–1807, Aug. 2020, doi: 10.1109/TNSRE.2020.3003559.
- [17] M. Viceconti, C. Curreli, F. Bottin, and G. Davico, "Effect of suboptimal neuromuscular control on the risk of massive wear in total knee replacement," *Ann. Biomed. Eng.*, vol. 49, no. 12, pp. 3349–3355, Dec. 2021, doi: 10.1007/s10439-021-02795-y.
- [18] M. Amankwah, A. Bersani, D. Calvetti, G. Davico, E. Somersalo, and M. Viceconti, "Exploring muscle recruitment by Bayesian methods during motion," *Chaos, Solitons Fractals*, vol. 185, Aug. 2024, Art. no. 115082, doi: 10.1016/j.chaos.2024.115082.
- [19] B. J. Fregly et al., "Grand challenge competition to predict in vivo knee loads," J. Orthopaedic Res., vol. 30, no. 4, pp. 503–513, Apr. 2012, doi: 10.1002/jor.22023.
- [20] B. van Veen, E. Montefiori, L. Modenese, C. Mazza, and M. Viceconti, "Muscle recruitment strategies can reduce joint loading during level walking," *J. Biomechanics*, vol. 97, Dec. 2019, Art. no. 109368, doi: 10.1016/j.jbiomech.2019.109368.
- [21] S. L. Delp et al., "OpenSim: Open-source software to create and analyze dynamic simulations of movement," *IEEE Trans. Biomed. Eng.*, vol. 54, no. 11, pp. 1940–1950, Nov. 2007, doi: 10.1109/TBME.2007. 901024.
- [22] R. D. Crowninshield and R. A. Brand, "A physiologically based criterion of muscle force prediction in locomotion," *J. Biomechanics*, vol. 14, no. 11, pp. 793–801, Jan. 1981, doi: 10.1016/0021-9290(81)90035-X.
- [23] D. C. Lin, C. P. McGowan, K. P. Blum, and L. H. Ting, "Yank: The time derivative of force is an important biomechanical variable in sensorimotor systems," *J. Experim. Biol.*, vol. 222, no. 18, Sep. 2019, Art. no. jeb180414, doi: 10.1242/jeb.180414.
- [24] P. Del Moral, Feynman-Kac Formulae (Probability and Its Applications). New York, NY, USA: Springer, 2004, doi: 10.1007/978-1-4684-9393-1.
- [25] K. Martinopoulou, O. Donti, W. Sands, G. Terzis, and G. Bogdanis, "Evaluation of the isometric and dynamic rates of force development in multi-joint muscle actions," *J. Human Kinetics*, vol. 81, pp. 135–148, Feb. 2022, doi: 10.2478/hukin-2021-0130.
- [26] S. H. Collins and A. D. Kuo, "Two independent contributions to step variability during over-ground human walking," *PLoS ONE*, vol. 8, no. 8, Aug. 2013, Art. no. e73597, doi: 10.1371/journal.pone.0073597.
- [27] G. Davico, L. Labanca, I. Gennarelli, M. G. Benedetti, and M. Viceconti, "Towards a comprehensive biomechanical assessment of the elderly combining in vivo data and in silico methods," Frontiers Bioeng. Biotechnol., vol. 12, May 2024, Art. no. 1356417, doi: 10.3389/fbioe.2024.1356417.
- [28] L. L. Andersen and P. Aagaard, "Influence of maximal muscle strength and intrinsic muscle contractile properties on contractile rate of force development," *Eur. J. Appl. Physiol.*, vol. 96, no. 1, pp. 46–52, Jan. 2006, doi: 10.1007/s00421-005-0070-z.
- [29] T. Kamo et al., "Rate of torque development and the risk of falls among community dwelling older adults in Japan," *Gait Posture*, vol. 72, pp. 28–33, Jul. 2019, doi: 10.1016/j.gaitpost.2019.05.019.
- [30] D. P. LaRoche, K. A. Cremin, B. Greenleaf, and R. V. Croce, "Rapid torque development in older female fallers and nonfallers: A comparison across lower-extremity muscles," *J. Electromyogr. Kinesiol.*, vol. 20, no. 3, pp. 482–488, Jun. 2010, doi: 10.1016/j.jelekin.2009.08.004.
- [31] T. B. Palmer, R. M. Thiele, E. C. Conchola, D. B. Smith, and B. J. Thompson, "A preliminary study of the utilization of maximal and rapid strength characteristics to identify chair-rise performance abilities in very old adults," *J. Geriatric Phys. Therapy*, vol. 39, no. 3, pp. 102–109, Jul. 2016, doi: 10.1519/jpt.0000000000000000.
- [32] E. Sundstrup et al., "Muscle function and postural balance in lifelong trained male footballers compared with sedentary elderly men and youngsters," Scandin. J. Med. Sci. Sports, vol. 20, no. 1, pp. 90–97, Apr. 2010, doi: 10.1111/j.1600-0838.2010.01092.x.
- [33] B. Kirking, J. Krevolin, C. Townsend, C. W. Colwell, and D. D. D'Lima, "A multiaxial force-sensing implantable tibial prosthesis," *J. Biomechanics*, vol. 39, no. 9, pp. 1744–1751, 2006, doi: 10.1016/j.jbiomech.2005.05.023.